Head-to-Head Comparison of ^{68}Ga-PSMA-11 PET/CT and mpMRI with a Histopathology Gold Standard in the Detection, Intraprostatic Localization, and Determination of Local Extension of Primary Prostate Cancer: Results from a Prospective Single-Center Imaging Trial

Ida Sonni[1], Ely R. Felker[2], Andrew T. Lenis[3], Anthony E. Sisk[4], Shadfar Bahri[1,5], Martin Allen-Auerbach[1,5], Wesley R. Armstrong[1], Voraparee Suvannarerg[2,6], Teeravut Tubtawee[2,7], Tristan Grogan[8], David Elashoff[8], Matthias Eiber[1,9], Steven S. Raman[2], Johannes Czernin[1,5,10], Robert E. Reiter*[3,5,10], and Jeremie Calais*[1,5,10]

[1]Ahmanson Translational Theranostics Division, Department of Molecular and Medical Pharmacology, David Geffen School of Medicine, UCLA, Los Angeles, California; [2]Department of Radiology, David Geffen School of Medicine, UCLA, Los Angeles, California; [3]Department of Urology, UCLA, Los Angeles, California; [4]Department of Pathology, David Geffen School of Medicine, UCLA, Los Angeles, California; [5]Institute of Urologic Oncology, David Geffen School of Medicine, UCLA, Los Angeles, California; [6]Department of Radiology, Faculty of Medicine, Siriraj Hospital, Mahidol University, Bangkok, Thailand; [7]Department of Radiology, Prince of Songkla University, Hat Yai, Thailand; [8]Department of Medicine Statistics Core, UCLA, Los Angeles, California; [9]Department of Nuclear Medicine, Klinikum Rechts der Isar, Technical University of Munich, Munich, Germany; and [10]Jonsson Comprehensive Cancer Center, UCLA, Los Angeles, California

The role of prostate-specific membrane antigen (PSMA)–targeted PET in comparison to multiparametric MRI (mpMRI) in the evaluation of intraprostatic cancer foci is not well defined. The aim of our study was to compare the diagnostic performance of ^{68}Ga-PSMA-11 PET/CT (PSMA PET/CT), mpMRI, and PSMA PET/CT + mpMRI using 3 independent masked readers for each modality and with histopathology as the gold standard in the detection, intraprostatic localization, and determination of local extension of primary prostate cancer. **Methods:** Patients with intermediate- or high-risk prostate cancer who underwent PSMA PET/CT as part of a prospective trial (NCT03368547) and mpMRI before radical prostatectomy were included. Each imaging modality was interpreted by 3 independent readers who were unaware of the other modality result. A central majority rule was applied (2:1). Pathologic examination of whole-mount slices was used as the gold standard. Imaging scans and whole-mount slices were interpreted using the same standardized approach on a segment level and a lesion level. A "neighboring" approach was used to define imaging–pathology correlation for the detection of individual prostate cancer foci. Accuracy in determining the location, extraprostatic extension (EPE), and seminal vesicle invasion (SVI) of prostate cancer foci was assessed using receiver-operating-characteristic curve analysis. Interreader agreement was calculated using intraclass correlation coefficient analysis. **Results:** The final analysis included 74 patients (14 [19%] with intermediate risk and 60 [81%] with high risk). The cancer detection rate (lesion-based analysis) was 85%, 83%, and 87% for PSMA PET/CT, mpMRI, and PSMA PET/CT + mpMRI, respectively. The change in AUC was statistically significant between PSMA PET/CT + mpMRI and the 2 imaging modalities alone for delineation of tumor localization (segment-based analysis) ($P < 0.001$) but not between PSMA PET/CT and mpMRI ($P = 0.093$). mpMRI outperformed PSMA PET/CT in detecting EPE ($P = 0.002$) and SVI ($P = 0.001$). In the segment-level analysis, intraclass correlation coefficient analysis showed moderate reliability among PSMA PET/CT and mpMRI readers using a 5-point Likert scale (range, 0.53–0.64). In the evaluation of T staging, poor reliability was found among PSMA PET/CT readers and poor to moderate reliability was found for mpMRI readers. **Conclusion:** PSMA PET/CT and mpMRI have similar accuracy in the detection and intraprostatic localization of prostate cancer foci. mpMRI performs better in identifying EPE and SVI. For the T-staging evaluation of intermediate to high-risk prostate cancer, mpMRI should still be considered the imaging modality of reference. Whenever available, PSMA PET/MRI or the coregistration or fusion of PSMA PET/CT and mpMRI (PSMA PET/CT + mpMRI) should be used as it improves tumor extent delineation.

Key Words: PSMA PET/CT; prostate cancer; mpMRI; staging; T staging

J Nucl Med 2022; 63:847–854
DOI: 10.2967/jnumed.121.262398

Prostate cancer is the most common solid-organ malignancy in men, accounting for over 190,000 new diagnoses and over 33,000 deaths in 2020 (*1*). Distant extrapelvic staging in patients with unfavorable intermediate- and high-risk disease with cross-sectional imaging and bone scanning is recommended to guide initial therapy (*2,3*).

Current methods used to locally stage prostate cancer and identify the precise location of foci of disease rely on the results of systematic or targeted biopsies and multiparametric MRI (mpMRI). Although targeted biopsies have considerably improved the identification of clinically significant prostate cancer and even allowed for the tracking of biopsy cores over time, there is still over a 30% chance of missing

Received Apr. 18, 2021; revision accepted Sep. 26, 2021.
For correspondence or reprints, contact Ida Sonni (isonni@mednet.ucla.edu).
*Contributed equally to this work.
Guest Editor: Todd Peterson, Vanderbilt University
Published online Oct. 14, 2021.

clinically significant prostate cancer in men with multifocal disease (*4*). Further, in a cohort of men selected as candidates for focal therapy who underwent radical prostatectomy, nearly half had unidentified bilateral disease and would have been inadequately treated (*5*). Therefore, additional and perhaps complementary methods are needed to better characterize and identify clinically significant prostate cancer foci.

Prostate-specific membrane antigen (PSMA) is a transmembrane cell-surface protein overexpressed in prostate cancer cells relative to most other tissues (*6*). ^{68}Ga-PSMA-11 PET/CT (PSMA PET/CT) has been shown in prospective studies to be highly sensitive and specific for the identification of biochemically recurrent disease and to improve staging in patients with newly diagnosed disease (*7–9*). Previous studies comparing PSMA PET and mpMRI in the local staging of prostate cancer had overall discordant results. Although some studies found PSMA PET/CT to be superior to mpMRI (*10–12*), others showed no significant differences (*13,14*).

The goal of the current analysis was to compare the diagnostic performance of PSMA PET/CT, mpMRI, and the combination of the two (PSMA PET/CT + mpMRI) in the detection, intraprostatic localization, and determination of local extension of primary prostate cancer, with histopathology as the gold standard, using 3 masked independent readers for each modality.

MATERIALS AND METHODS

Study Design and Patient Population

We report here the results of an exploratory endpoint of a prospective trial conducted at UCLA (NCT03368547). The primary outcome of the trial was to evaluate the diagnostic performance (sensitivity, specificity, positive predictive value, and negative predictive value) of PSMA PET/CT for the detection of regional nodal metastases compared with histopathology at radical prostatectomy in patients with intermediate- to high-risk prostate cancer. The results of the primary endpoint analysis were the foundation of a new-drug application for ^{68}Ga-PSMA-11 (*15*) and will be reported separately.

For the current study, patients with biopsy-proven intermediate- or high-risk prostate cancer by NCCN (*16*) and enrolled in the pivotal trial were included in the analysis if they underwent initial staging with both PSMA PET/CT and mpMRI at our institution and subsequently underwent radical prostatectomy. Patients treated with androgen deprivation therapy were excluded from the analysis. The study was done under an investigational-new-drug approval protocol (IND 130649) and was approved by the local institutional review board (approval 16-001684).

mpMRI Image Acquisition

mpMRI was performed on a 3-T MRI system (Magnetom Trio, Skyra, or Verio; Siemens Medical Systems) using a standardized protocol with pelvic external phased-array coils. The mpMRI protocol included conventional multiplanar T2-weighted turbo spin-echo imaging, diffusion-weighted imaging, axial unenhanced T1-weighted imaging, and axial 3-dimensional fast-field echo dynamic contrast-enhanced imaging, as described previously (*17*). In addition, a small–field-of-view 3-dimensional axial turbo spin-echo T2-weighted sequence was performed using spatial and chemical-shift encoded excitation (SPACE; Siemens Healthcare), as described in detail previously (*17,18*).

PSMA PET/CT Image Acquisition

PSMA PET/CT images were acquired after intravenous injection of a median of 192.4 MBq of ^{68}Ga-PSMA-11 (interquartile range, 185–203.5 MBq) and a median uptake time of 61.5 min (interquartile range, 58–67 min) using a Biograph 64 or mCT PET/CT scanner (Siemens Medical Systems) (axial field of view, 22.1 cm). ^{68}Ga-PSMA-11 (Glu-NH-CO-NH-Lys-(Ahx)-[^{68}Ga(HBEDCC)]) was used as the PSMA ligand (*19*) and was obtained from the Biomedical Cyclotron Facility at UCLA. Oral and intravenous CT contrast media were administered unless contraindicated. A 5-mm slice thickness was used for the CT scan. All PET images acquired from pelvis to vertex were corrected for attenuation, dead time, random events, and scatter. The time per bed position was based on patient weight (*20*).

Image Analysis

For the purpose of this exploratory endpoint analysis, the PSMA PET/CT and mpMRI were read independently by 3 board-certified nuclear medicine physicians (with 4, 4, and 1 y of experience in interpreting PSMA PET/CT, that is, ~250 scans/y, and 19, 7, and 7 y of experience in interpreting oncologic PET/CT, that is, ~1,000 scans/y) and 3 radiologists (with 5, 5, and 12 y of experience in prostate mpMRI, that is, ~1,000 scans/y) using OsiriX and DynaCAD software, respectively (*21*).

All readers were aware of the presence of biopsy-proven prostate cancer but not of any other demographic, clinical, pathology, or imaging information. The readers were masked to the PSMA PET/CT and mpMRI clinical reports and to the other readers' findings. A standardized approach was used for imaging interpretation, assessing the presence, location, and size of prostate cancer foci (lesions) within the prostate. The analysis was conducted on an individual-lesion level and on a segment level.

Segment-Level Analysis (Prostate Cancer Localization). The prostate was divided into 12 segments using orthogonal axial planes for PSMA PET/CT and oblique axial planes for mpMRI: base, mid gland, and apex, defined as the upper, middle, and lower thirds, respectively, of the prostate; right/left and anterior/posterior were defined on axial views by a vertical line (sagittal plane) and horizontal line (coronal plane), respectively, passing through the center of the prostate (Fig. 1). The 12 segments used in this analysis represented a compromise between the 41 sectors used in the Prostate Imaging Reporting and Data System (PI-RADS) score and the sextants used for PSMA PET in previous studies (*12,22*). All PSMA PET/CT and mpMRI readers assigned each segment a score using a 5-point Likert scale (PSMA score, resembling scores using PSMA-RADS version 1.0 (*23,24*) and PI-RADS version 2.1 (*25*), respectively) based on the overall likelihood of prostate cancer. Each reader's 5-point scores were further converted into a binary score (1 and 2 = negative for cancer; 3, 4, and 5 = positive for cancer).

Lesion-Level Analysis (Prostate Cancer Detection). A maximum of 3 prostate cancer lesions was listed for each patient and described as the index, secondary, and tertiary lesions. Each reader recorded lesion size and other parameters (i.e., SUV_{max} for PSMA PET/CT and diffusion-weighted imaging PI-RADS score for mpMRI) to aid in the overall interpretation.

T Staging. The presence of bilateral intraprostatic disease, seminal vesicle invasion (SVI [T3b]), and extraprostatic extension (EPE [T3a]) was assessed visually in a binary manner (*26*).

Majority Rule and Central Reads. One lead investigator collected the imaging and pathology reads and conducted the final analysis. A central majority rule (2:1) was used to obtain the final reads for PSMA PET/CT and mpMRI. On a segment level, lesion level, and T-staging level, positivity for cancer involvement in the individual segment, lesion, or T level was considered present if at least 2 of 3 readers described it as positive for cancer.

PSMA PET/CT + mpMRI. PSMA PET/CT + mpMRI findings were obtained by combining the central majority reads from the 2 imaging modalities. If a segment, lesion, or T-level finding was described as positive on only 1 imaging modality (only on PET or mpMRI), it was automatically considered positive on PSMA PET/CT + mpMRI.

Histopathology Analysis

Whole-mount slices (tissue sections of 5 mm, histologic sections cut at 5 μm) were read by a genitourinary pathologist (with 7 y of whole-mount

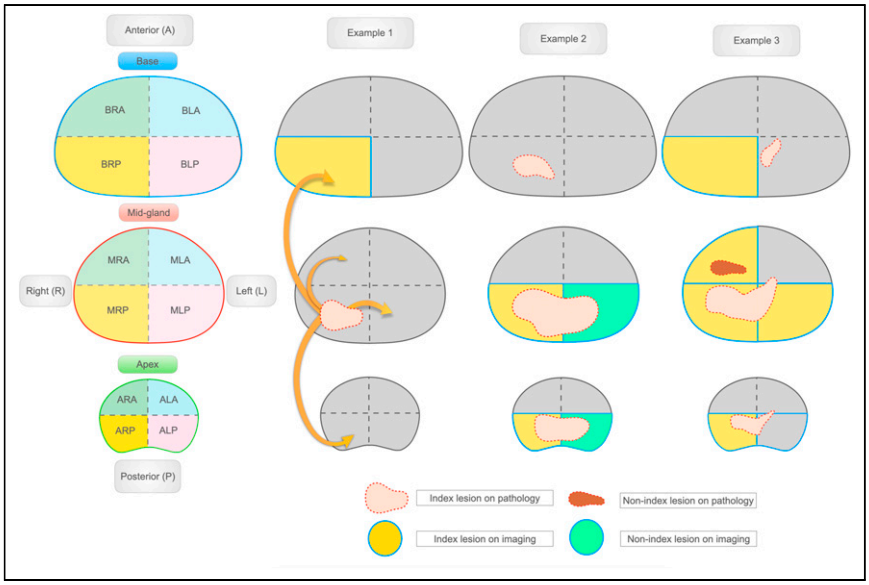

FIGURE 1. Prostate segmentation template and imaging–pathology correspondence for lesion-based analysis. Twelve-segment subdivision of prostate gland was used for standardized reads (left). Examples are shown of imaging–pathology correlation for lesion-level analysis using neighboring approach. Arrows indicate adjacent or neighboring segments. (Example 1) One lesion described on pathology as involving segment MRP, and 1 lesion identified by imaging as involving segment BRP. Imaging–pathology correlation: true-positive finding because BRP and MRP are neighboring segments. (Example 2) One large lesion described on pathology as involving segments ARP, MRP, BRP, ALP, and MLP, and 2 lesions identified by imaging (lesion 1, involving ARP and MRP [yellow segments], and lesion 2, involving ALP and MLP [green segments]). Imaging–pathology correlation: true-positive because one single lesion was described on pathology and correctly identified as cancer by imaging, even though described differently. (Example 3) Two lesions described on pathology (lesion 1, involving ALP, MLP, BLP, ALA, MLA, ARP, and MRP [pink lesion], and lesion 2, involving MRA [red lesion]), and 1 large lesion described by imaging as involving segments ARP, MRP, MLP, BRP, and MRA. Imaging–pathology correlation: 2 true-positive findings because 2 lesions were described on pathology, and both were described as cancer on imaging.

experience) who was masked to all imaging results using the lesion- and segment-level approach. Each lesion was assessed for the presence, location, and size of cancer foci and for the Gleason grade.

Benign prostatic lesions were not considered and were excluded from the detection analysis.

Imaging–Pathology Correlation

To define imaging–pathology correspondence on a lesion level, an adaptation of a previously described approach was used (Fig. 1) (*27*). This "neighboring" approach did not take into account the number of lesions and allowed the location correspondence to involve the immediately adjacent segments. This approach was used to overcome possible interpretation errors due to misregistration or misalignment deriving from deformation and shrinkage during fixation, commonly happening during whole-mount slice preparation (*28*), or due to use of different orientations by PSMA PET/CT, mpMRI, and pathologic examination of whole-mount slices (prostatectomy specimen cross section) to define the prostate base, mid-gland, and apical regions.

Statistical Analysis

Patient characteristics and study variables were summarized using mean and SD, median and interquartile range, or frequency and percentage, as appropriate. The diagnostic performance of PSMA PET/CT, mpMRI, and PSMA PET/CT + mpMRI were compared with histopathologic analysis on a lesion level and a segment level. Receiver-operating-characteristic curves and area under the receiver-operating-characteristic curves (AUCs) were obtained along with 95% CIs. AUC CI changes and *P* values were determined using the DeLong test.

Interrater agreement was calculated using the intraclass correlation coefficient (ICC) with the 2-way random-effects model, using absolute-agreement and single-measure options. Statistical analyses were performed using SPSS (version 25; IBM), and *P* values of less than 0.05 were considered statistically significant.

RESULTS

Patient Population

Between January 2017 and November 2019, 398 patients were enrolled in the trial. Seventy-four patients were included in the final analysis of this study (study flowchart in Fig. 2). The mean time was 43 d (SD, 39.9 d; range, −31 to 123 d) between PSMA PET/CT and mpMRI, 54.1 d (SD, 35.9 d; range, 6–180 d) between PSMA PET/CT and radical prostatectomy, and 100.8 d (SD, 53.4 d; range, 3–288 d) between mpMRI and radical prostatectomy. In 44 of 74 patients (59%), the mpMRI was performed before the biopsy, whereas all PSMA PET/CT scans were obtained after confirmation of a positive biopsy. Patient characteristics are summarized in Table 1.

Prostate Cancer Localization (Segment-Based Analysis)

In total, 425 of 888 segments (48%) were positive for cancer by pathologic examination. PSMA PET/CT, mpMRI, and PSMA PET/CT + mpMRI found cancer (majority reads) in 310 (35%), 314 (35%), and 405 (46%) segments, respectively. The results of the segment-level analysis and the receiver-operating-characteristic curve analysis per reader and per imaging modality are shown in Figures 3A and 3B. In total, 408 of 888 segments (46%) were described as harboring clinically significant prostate cancer (Gleason score $> 3 + 3 = 6$). The results of a subanalysis including only clinically significant lesions are shown in Supplemental Figure 1 (supplemental materials are available at http://jnm.snmjournals.org).

The AUCs for PSMA PET/CT, mpMRI, and PSMA PET/CT + mpMRI were 0.7 (sensitivity, 0.84; specificity, 0.55), 0.73 (sensitivity, 0.86; specificity, 0.59), and 0.77 (sensitivity, 0.77; specificity, 0.71), respectively. The change in AUC was statistically significant between PSMA PET/CT + mpMRI and the 2 imaging modalities alone ($P < 0.001$) but not between PSMA PET/CT and mpMRI ($P = 0.093$).

The AUCs for readers 1, 2, and 3 were 0.69, 0.69, and 0.66, respectively, using the PSMA score and 0.71, 0.72, and 0.71, respectively, using the PI-RADS score.

ICC analysis showed moderate reliability (*29*) among PSMA PET/CT and mpMRI readers using the 5-point Likert scale (PSMA PET/CT: reader 1/reader 2, 0.63; reader 1/reader 3, 0.53; and reader 2/reader 3, 0.64) (mpMRI: reader 1/reader 2, 0.61; reader 1/reader 3, 0.55; and reader 2/reader 3, 0.55).

Prostate Cancer Detection (Lesion-Based Analysis)

Pathologic examination of whole-mount slices identified 109 prostate cancer foci (74, 32, and 3 index, secondary, and tertiary lesions, respectively). Using the majority reads, PSMA PET/CT

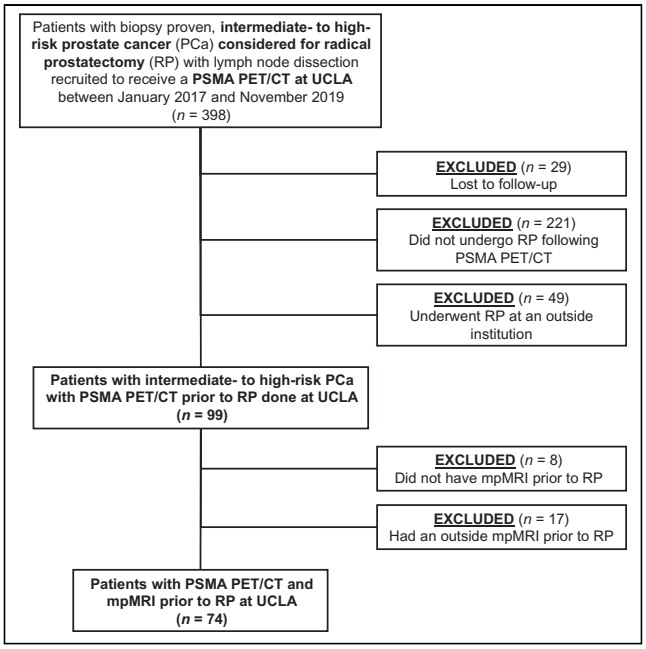

FIGURE 2. Study flowchart.

identified 111 lesions (74, 33, and 4 index, secondary, and tertiary lesions, respectively) and mpMRI identified 91 (74, 16, and 1 index, secondary, and tertiary lesions, respectively). The results of the lesion-level analysis and detection rates for all cancerous lesions are shown in Table 2. Individual readers' results are shown in Supplemental Table 1.

The detection rate was 85%, 83%, and 87% for PSMA PET/CT, mpMRI, and PSMA PET/CT + mpMRI, respectively. PSMA PET/CT identified 4 lesions (1 primary and 3 secondary) missed by mpMRI, whereas mpMRI identified 2 lesions (1 primary and 1 secondary) missed by PSMA PET/CT (Supplemental Table 2). Differences in detection rates between PSMA PET/CT and mpMRI were not statistically significant. The addition of PSMA PET/CT did not provide significant increases in detection rates over mpMRI alone.

Two separate subanalyses excluding small cancerous lesions (≤0.5 cm on histopathologic analysis) and lesions with a Gleason score of 3 + 3 = 6 were conducted.

Twelve of 109 lesions (11%) were graded as having a Gleason score of 3 + 3 = 6 (10 secondary lesions and 2 tertiary lesions). The overall detection rate excluding these lesions was 95% for PSMA PET/CT + mpMRI (vs. 92% for both PSMA PET/CT and mpMRI alone).

The detection rates for clinically significant lesions are summarized in Table 2.

Five of 109 lesions (5%) measured 0.5 cm or less on histopathologic analysis. Three of the 5 were not detected by either imaging modality, 1 of the 5 was identified by both, and 1 of the 5 was identified by mpMRI and PSMA PET/CT.

Figure 4 and Supplemental Figure 2 show examples of a PSMA PET/CT image, an mpMRI image, and a whole-mount slice from our cohort.

T Staging

Histopathologic examination detected bilateral disease in 37 of 74 patients (50%), SVI in 25 of 74 (34%), and EPE in 43 of 74 (58%). By majority reads, although mpMRI had a higher AUC than PSMA PET/CT for the detection of bilateral disease (0.65 vs. 0.54), this difference was not significantly different (DeLong test, $P = 0.138$) (Fig. 3). mpMRI had a better AUC than PSMA PET/CT for detection of EPE (0.79 vs. 0.59, $P = 0.002$) or SVI (0.84 vs. 0.63, $P = 0.001$). The use of PSMA PET/CT + mpMRI did not provide statistically significantly improvements over mpMRI alone.

Poor reliability was found among readers for PSMA PET/CT in the evaluation of bilaterality (ICC, 0.344), EPE (ICC, 0.203), and SVI (ICC, 0.081); moderately strong reliability was found among mpMRI readers for bilaterality (ICC, 0.693) and EPE (ICC, 0.580), and poor reliability was found for SVI (ICC, 0.305).

TABLE 1
Patient Characteristics

Characteristic	Data
No. of patients	74
Median age (y)	65 (IQR, 60–69)
Median PSA (ng/mL)	11.1 (IQR, 7.5–21.5)
Initial PSA (ng/mL)	
<10	29 (39%)
10–20	26 (35%)
>20	19 (26%)
D'Amico risk classification	
Intermediate risk	14 (19%)
High risk	60 (81%)
Presurgical Gleason grade	
3 + 3 = 6	1 (1%)
3 + 4 = 7	14 (20%)
3 + 5 = 8	2 (2%)
4 + 3 = 7	13 (19%)
4 + 4 = 8	24 (34%)
4 + 5 = 9	19 (27%)
5 + 4 = 9	1 (1%)

IQR = interquartile range; PSA = prostate-specific antigen level.

DISCUSSION

Using the majority reads of 3 masked independent readers for each imaging modality, our single-center study including 74 patients with intermediate- to high-risk prostate cancer found that PSMA PET/CT and mpMRI performed similarly in the detection and intraprostatic localization of primary prostate cancer, whereas mpMRI was superior for determining the T stage. The combined use of PSMA PET/CT and mpMRI improved tumor extent delineation (segment-level analysis) and allowed the identification of multifocal lesions but did not significantly improve the detection rates (lesion-level analysis) of the 2 modalities alone.

Current clinical guidelines (*2,30*) still recommend the use of cross-sectional imaging (CT or MRI) with bone scanning for extraprostatic distant staging in patients with intermediate- to high-risk prostate cancer. Several studies showed PSMA PET/CT to be superior to conventional imaging in the evaluation of N and M stage (*7–9,31–34*), but its added value in the definition of

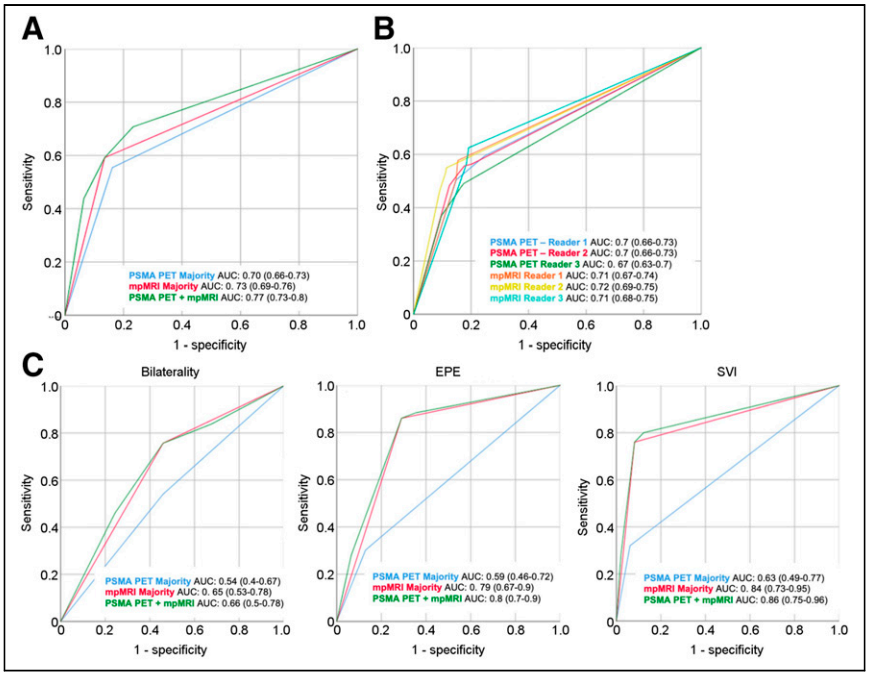

FIGURE 3. Prostate cancer localization (segment-based analysis) and T3 staging. (A and B) Receiver-operating-characteristic curves for segment-level analysis obtained for PSMA PET/CT and mpMRI majority reads (A) and using 1–5 PSMA and PI-RADS score for each individual reader (B). Graphs show change in AUC between PSMA PET/CT and mpMRI (95% CI, −0.01 to 0.07; P = 0.093), between PSMA PET/CT + mpMRI and PSMA PET/CT (95% CI, 0.05–0.1; $P < 0.001$), and between PSMA PET/CT + mpMRI and mpMRI (95% CI, 0.03–0.06; $P < 0.001$). (C) Receiver-operating-characteristic curves for PSMA PET/CT and mpMRI majority reads in evaluation of T staging. Graphs show change in AUC for bilateral disease (0.65 vs. 0.54, DeLong test, P = 0.138), change in AUC for EPE (0.79 vs. 0.59; 95% CI, 0.08–0.32; P = 0.002), and change in AUC for SVI (0.84 vs. 0.63; 95% CI, 0.09–0.33; P = 0.001).

T stage and in intraprostatic tumor localization is still controversial. The goal of our analysis was to compare the 2 imaging modalities in the definition of local disease and to evaluate whether the combination of the two provides any significant advantage. In this setting, the current literature shows discordant results, mostly due to small cohorts, different study designs, and different approaches in defining the imaging–pathology correlation. Unlike previous studies, the current work included a relatively large cohort of prospectively selected patients and involved a standardized approach to the correlation analysis of image findings and whole-mount pathology findings. An additional analysis on T staging was conducted, as well as a subanalysis on lesions with lower Gleason grades (3 + 3 = 6). In our study, PSMA PET/CT allowed the detection of 4 lesions missed by mpMRI (4/109 lesions [4%]) but also misclassified more lesions as prostate cancer (higher number of false-positives) at the expense of the positive predictive value. In a future study, we will conduct an additional analysis specifically looking at lesions negative on both imaging modalities, discordant cases, and the histopathologic features of these tumor foci.

The segment-level analysis for localization of prostate cancer foci did not show significant differences between PSMA PET/CT and mpMRI. Conversely, the addition of PSMA PET/CT to mpMRI significantly increased the number of segments detected, indicating that PSMA PET/CT improves the definition of tumor extent and can be an important aid in guiding the initial therapeutic approach (*5*). However, to confirm this finding, further investigation is needed.

The results were obtained using a neighboring approach to evaluate imaging–pathology correlation, which was applied to overcome the intrinsic limitation of the lack of registration between imaging and pathology. The use of PSMA PET/CT + mpMRI allowed the detection of 99% of primary lesions and 69% of secondary lesions, with an overall detection rate of 87% (vs. 85% and 83% for PSMA PET/CT and mpMRI alone, respectively) for all lesions, and 95% (vs. 92% for both PSMA PET/CT and mpMRI alone) for clinically significant lesions (Supplemental Table 2). On the basis of the improved performance of the combined PSMA PET/CT + mpMRI information, we recommend that discordant cases in clinical practice be evaluated in consensus between PET/CT and MRI readers or by a multidisciplinary prostate cancer tumor board. A lesion detected on only one of the modalities should be considered suggestive of cancer. Whenever possible, the PSMA PET/CT and mpMRI images should be coregistered using the CT and MRI prostate contours as a reference.

mpMRI performed significantly better than PSMA PET/CT in the definition of T stage, that is, SVI (T3b) and EPE (T3a), but not in the detection of bilateral disease (T2c). This finding is attributable mainly to the poor interreader agreement among the 3 PET readers for T staging, probably because of the lack of standardized criteria for T-staging evaluation by PSMA PET/CT. In contrast, since the correct definition of the locoregional extension of prostate cancer relies strongly on visualization of anatomic detail, the well-established higher soft-tissue contrast, higher spatial resolution, and multiplanar capability of mpMRI represent an advantage over CT and led to good agreement among the 3 MRI readers for T staging. However, interrater reliability was also poor for mpMRI readers in the evaluation of SVI. These results contrast with those of a previously published study involving 54 patients; in that study, PSMA PET/CT showed a higher sensitivity for the definition of EPE but not for SVI (*35*).

Intraprostatic tumor detection and localization by PSMA PET/CT relies largely on the PSMA PET signal because of the poor tissue contrast of CT. Consequently, lesion localization is highly dependent on the SUV visual scaling threshold used while interpreting the scans. The readers did not receive any specific recommendation on a fixed SUV threshold, as interpretation should be done by adapting the scaling to the background signal. This lack of a recommendation represents a source of interreader variability, but despite this inherent limitation for PSMA PET/CT, the segment-level analysis for localization of prostate cancer foci did not show significant differences from mpMRI.

Several studies showed that the combined use of PSMA PET/CT and mpMRI provides the best diagnostic accuracy overall (*10,14*). In light of the recent advent of PET/MRI, a growing body of literature is now available using PSMA PET/MRI, which has been shown by several groups to outperform each modality alone (*22,28,36–38*). However, the limited number of PET/MRI scanners available worldwide

TABLE 2
Prostate Cancer Detection Rates (Lesion-Based Analysis)

Parameter	All lesions			Clinically significant lesions		
	PSMA PET/CT	mpMRI	PSMA PET/CT + mpMRI	PSMA PET/CT	mpMRI	PSMA PET/CT + mpMRI
Index lesion (n = 74)	72 (97%)	72 (97%)	73 (99%)	72 (97%)	72 (97%)	73 (99%)
Secondary lesion (n = 32)	21 (66%)	19 (59%)	22 (69%)	18 (81%)	18 (81%)	19 (86%)
Tertiary lesion (n = 3)	0 (0%)	0 (0%)	0 (0%)	0 (0%)	0 (0%)	0 (0%)
Overall (detection rate)	93 (85%)	91 (83%)	95 (87%)	90 (93%)	90 (93%)	92 (95%)
Positive predictive value	97%	100%	—	94%	100%	—

Clinically significant lesions exclude lesions with Gleason score of 3 + 3 = 6. Differences in detection rate between PSMA PET/CT and mpMRI were not statistically significant.

and the associated high costs still limit its widespread use in clinical practice. The well-established superiority of PSMA PET/CT in N and M staging, combined with an enhanced ability to determine T stage and local extension with mpMRI, highlights the complementary role of each imaging modality and underscores the diagnostic potential of PSMA PET/MRI. If available, PSMA PET/MRI should be considered the modality of choice in the initial evaluation of patients with advanced prostate cancer. When a hybrid PET/MRI scanner is not available, the PSMA PET/CT and mpMRI images acquired separately should be coregistered using a reproducible multimodality DICOM image-fusion tool. If this is not possible, mpMRI remains the imaging modality of reference for the evaluation of T stage.

The main limitations of the study are the lack of coregistration between PSMA PET/CT, mpMRI, and pathology and the absence of the use of a 3-dimensional custom mold (*39–41*). To compensate for this inaccurate imaging–pathology correlation, we used a neighboring approach. Another limitation is that the interval between mpMRI and radical prostatectomy was not homogeneous, ranging between 3 and 288 d, raising the potential issue of inherent tumor changes over time. Additionally, sources of bias include the lack of negative controls in the cohort, as all imaging readers were aware of the presence of biopsy-proven high- to intermediate-risk prostate cancer, and patient selection, as we cannot rule out the exclusion of patients with a positive mpMRI result and a negative biopsy result from the final cohort. Thus, the PPV should be interpreted with caution. Finally, since we included only patients with intermediate- and high-risk disease, we were not able to address the clinical question of whether PSMA PET/CT can bring a significant added value to mpMRI in the initial staging of a heterogeneous population of patients with prostate cancer, including patients with less aggressive disease.

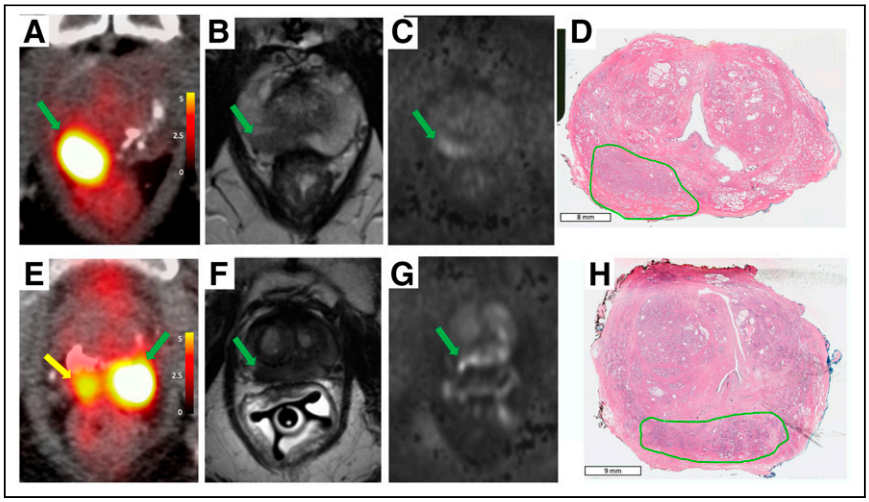

FIGURE 4. Two case examples from our cohort. (A–D) A 68-y-old patient (patient 4) with biopsy-proven prostate cancer with Gleason score of 3 + 4 = 7 and PSA of 8.6 ng/mL at time of PSMA PET/CT. Transverse PSMA PET/CT image (A), T2-weighted MR image (B), and high b-value diffusion-weighted MR image (C) show right-posterior mid-gland lesion (arrows). Whole-mount slice (D) shows 1 lesion, with Gleason score of 4 + 3 = 7, in same segment (contoured in green), and lesion showed EPE. There was good imaging–pathology correspondence (true-positive finding for both imaging modalities). All 6 readers correctly identified and described lesion. (E–H) A 69-y-old patient (patient 5) with biopsy-proven prostate cancer with Gleason score of 3 + 4 = 7 and PSA of 11.4 ng/mL at time of PSMA PET/CT. Transverse PSMA PET/CT image (E) shows 2 foci of increased PSMA uptake in right-posterior apex (yellow arrow) and left-posterior apex (green arrow). PSMA reader 1 correctly described 1 lesion involving left- and right-posterior apex; PSMA readers 2 and 3 described left and right foci as 2 separate lesions. T2-weighted MR image (F) shows hypointense lesion, and diffusion-weighted image (G) shows diffusion restriction in right- and left-posterior apex (arrow). All MRI readers correctly described only 1 lesion. Whole-mount slice (H) shows 1 lesion encompassing both right- and left-posterior apex (contoured in green) with EPE. This is an example of same lesion being described differently by PSMA PET/CT and whole-mount slice (true-positive finding for both imaging modalities).

CONCLUSION

In our study using the majority reads of 3 masked independent readers for each modality, both PSMA PET/CT and mpMRI performed well in the detection and intraprostatic localization of intermediate- to high-risk primary prostate cancer, whereas mpMRI had superior performance in the definition of T stage (T2c, T3). The combined use of PSMA PET/CT and mpMRI improved tumor extent delineation. Our findings highlight the complementarity of the 2 imaging modalities.

DISCLOSURE

Johannes Czernin is a board member of Sofie Biosciences and a founder of Trethera Therapeutics. Jeremie Calais reports prior consulting activities outside the submitted work for Advanced Accelerator Applications, Blue Earth Diagnostics, Curium Pharma, GE Healthcare, Janssen, POINT Biopharma, Progenics, Radiomedix, and Telix Pharmaceuticals. He is the recipient of grants from the Prostate Cancer Foundation (2020 Young Investigator Award 20YOUN05), the Society of Nuclear Medicine and Molecular Imaging (2019 Molecular Imaging Research Grant for Junior Academic Faculty), the Philippe Foundation Inc. (New York, USA), and the ARC Foundation (France) (International Mobility Award SAE20160604150). No other potential conflict of interest relevant to this article was reported.

KEY POINTS

QUESTION: How does PSMA PET/CT perform in the local evaluation of primary prostate cancer in comparison to mpMRI, and is there an additional value in the combined use of both PSMA PET/CT and MRI in comparison to mpMRI alone?

PERTINENT FINDINGS: The 2 imaging modalities showed similar accuracy in the detection and localization of intraprostatic lesions, whereas mpMRI performed better in the definition of EPE and SVI. The combined use of the two leads to better cancer localization but did not significantly improve detection rates.

IMPLICATIONS FOR PATIENT CARE: In this study, the addition of PSMA PET/CT to mpMRI did not significantly change local staging in patients with intermediate- to high-risk prostate cancer.

REFERENCES

1. Siegel RL, Miller KD, Jemal A. Cancer statistics, 2020. *CA Cancer J Clin.* 2020; 70:7–30.
2. Mottet N, Bellmunt J, Bolla M, et al. EAU-ESTRO-SIOG guidelines on prostate cancer. Part 1: screening, diagnosis, and local treatment with curative intent. *Eur Urol.* 2017;71:618–629.
3. Sanda MG, Cadeddu JA, Kirkby E, et al. Clinically localized prostate cancer: AUA/ASTRO/SUO guideline. Part I: risk stratification, shared decision making, and care options. *J Urol.* 2018;199:683–690.
4. Johnson DC, Raman SS, Mirak SA, et al. Detection of individual prostate cancer foci via multiparametric magnetic resonance imaging. *Eur Urol.* 2019;75: 712–720.
5. Johnson DC, Yang JJ, Kwan L, et al. Do contemporary imaging and biopsy techniques reliably identify unilateral prostate cancer? Implications for hemiablation patient selection. *Cancer.* 2019;125:2955–2964.
6. Silver DA, Pellicer I, Fair WR, Heston WD, Cordon-Cardo C. Prostate-specific membrane antigen expression in normal and malignant human tissues. *Clin Cancer Res.* 1997;3:81–85.
7. Hofman MS, Lawrentschuk N, Francis RJ, et al. Prostate-specific membrane antigen PET-CT in patients with high-risk prostate cancer before curative-intent surgery or radiotherapy (proPSMA): a prospective, randomised, multicentre study. *Lancet.* 2020;395:1208–1216.
8. Hope TA, Goodman JZ, Allen IE, Calais J, Fendler WP, Carroll PR. Metaanalysis of ^{68}Ga-PSMA-11 PET accuracy for the detection of prostate cancer validated by histopathology. *J Nucl Med.* 2019;60:786–793.
9. Lenis AT, Pooli A, Lec PM, et al. Prostate-specific membrane antigen positron emission tomography/computed tomography compared with conventional imaging for initial staging of treatment-naïve intermediate- and high-risk prostate cancer: a retrospective single-center study. *Eur Urol Oncol.* September 18, 2020 [Epub ahead of print].
10. Rhee H, Thomas P, Shepherd B, et al. Prostate specific membrane antigen positron emission tomography may improve the diagnostic accuracy of multiparametric magnetic resonance imaging in localized prostate cancer. *J Urol.* 2016; 196:1261–1267.
11. Berger I, Annabattula C, Lewis J, et al. ^{68}Ga-PSMA PET/CT vs. mpMRI for locoregional prostate cancer staging: correlation with final histopathology. *Prostate Cancer Prostatic Dis.* 2018;21:204–211.
12. Donato P, Roberts MJ, Morton A, et al. Improved specificity with ^{68}Ga PSMA PET/CT to detect clinically significant lesions "invisible" on multiparametric MRI of the prostate: a single institution comparative analysis with radical prostatectomy histology. *Eur J Nucl Med Mol Imaging.* 2019; 46:20–30.
13. Kalapara AA, Nzenza T, Pan HYC, et al. Detection and localisation of primary prostate cancer using ^{68}gallium prostate-specific membrane antigen positron emission tomography/computed tomography compared with multiparametric magnetic resonance imaging and radical prostatectomy specimen pathology. *BJU Int.* 2020; 126:83–90.
14. Chen M, Zhang Q, Zhang C, et al. Combination of ^{68}Ga-PSMA PET/CT and multiparametric MRI improves the detection of clinically significant prostate cancer: a lesion-by-lesion analysis. *J Nucl Med.* 2019;60:944–949.
15. Gallium Ga 68 PSMA-11 injection, for intravenous use. Food and Drug Administration website. https://www.accessdata.fda.gov/drugsatfda_docs/label/2020/212642s000lbl.pdf. Published 2020. Revised December 2020. Accessed March 22. 2022.
16. Schaeffer E, Srinivas S, Antonarakis ES, et al. NCCN guidelines insights: prostate cancer, version 1.2021. *J Natl Compr Canc Netw.* 2021;19:134–143.
17. Tan N, Lin WC, Khoshnoodi P, et al. In-bore 3-T MR-guided transrectal targeted prostate biopsy: prostate imaging reporting and data system version 2-based diagnostic performance for detection of prostate cancer. *Radiology.* 2017;283:130–139.
18. Natarajan S, Marks LS, Margolis DJ, et al. Clinical application of a 3D ultrasound-guided prostate biopsy system. *Urol Oncol.* 2011;29:334–342.
19. Eder M, Schäfer M, Bauder-Wüst U, et al. ^{68}Ga-complex lipophilicity and the targeting property of a urea-based PSMA inhibitor for PET imaging. *Bioconjug Chem.* 2012;23:688–697.
20. Halpern BS, Dahlbom M, Quon A, et al. Impact of patient weight and emission scan duration on PET/CT image quality and lesion detectability. *J Nucl Med.* 2004; 45:797–801.
21. Rosset A, Spadola L, Ratib O. OsiriX: an open-source software for navigating in multidimensional DICOM images. *J Digit Imaging.* 2004;17:205–216.
22. Eiber M, Weirich G, Holzapfel K, et al. Simultaneous ^{68}Ga-PSMA HBED-CC PET/MRI improves the localization of primary prostate cancer. *Eur Urol.* 2016;70: 829–836.
23. Rowe SP, Pienta KJ, Pomper MG, Gorin MA. Proposal for a structured reporting system for prostate-specific membrane antigen-targeted PET imaging: PSMA-RADS version 1.0. *J Nucl Med.* 2018;59:479–485.
24. Rowe SP, Pienta KJ, Pomper MG, Gorin MA. PSMA-RADS version 1.0: a step towards standardizing the interpretation and reporting of PSMA-targeted PET imaging studies. *Eur Urol.* 2018;73:485–487.
25. Turkbey B, Rosenkrantz AB, Haider MA, et al. Prostate imaging reporting and data system version 2.1: 2019 update of prostate imaging reporting and data system version 2. *Eur Urol.* 2019;76:340–351.
26. Paner GP, Stadler WM, Hansel DE, Montironi R, Lin DW, Amin MB. Updates in the eighth ed. of the tumor-node-metastasis staging classification for urologic cancers. *Eur Urol.* 2018;73:560–569.
27. Turkbey B, Pinto PA, Mani H, et al. Prostate cancer: value of multiparametric MR imaging at 3 T for detection–histopathologic correlation. *Radiology.* 2010; 255:89–99.
28. Hicks RM, Simko JP, Westphalen AC, et al. Diagnostic accuracy of ^{68}Ga-PSMA-11 PET/MRI compared with multiparametric MRI in the detection of prostate cancer. *Radiology.* 2018;289:730–737.
29. Koo TK, Li MY. A guideline of selecting and reporting intraclass correlation coefficients for reliability research. *J Chiropr Med.* 2016;15:155–163.
30. Lam TBL, MacLennan S, Willemse PM, et al. EAU-EANM-ESTRO-ESUR-SIOG prostate cancer guideline panel consensus statements for deferred treatment with curative intent for localised prostate cancer from an international collaborative study (DETECTIVE study). *Eur Urol.* 2019; 76:790–813.
31. Kim SJ, Lee SW, Ha HK. Diagnostic performance of radiolabeled prostate-specific membrane antigen positron emission tomography/computed tomography for primary lymph node staging in newly diagnosed intermediate to high-risk prostate cancer patients: a systematic review and meta-analysis. *Urol Int.* 2019; 102:27–36.

32. Koschel S, Murphy DG, Hofman MS, Wong LM. The role of prostate-specific membrane antigen PET/computed tomography in primary staging of prostate cancer. *Curr Opin Urol.* 2019;29:569–577.
33. Perera M, Papa N, Roberts M, et al. Gallium-68 prostate-specific membrane antigen positron emission tomography in advanced prostate cancer: updated diagnostic utility, sensitivity, specificity, and distribution of prostate-specific membrane antigen-avid lesions—a systematic review and meta-analysis. *Eur Urol.* 2020;77:403–417.
34. Zacho HD, Nielsen JB, Haberkorn U, Stenholt L, Petersen LJ. ^{68}Ga-PSMA PET/CT for the detection of bone metastases in prostate cancer: a systematic review of the published literature. *Clin Physiol Funct Imaging.* October 29, 2017 [Epub ahead of print].
35. Chen M, Zhang Q, Zhang C, et al. Comparison of ^{68}Ga-prostate-specific membrane antigen (PSMA) positron emission tomography/computed tomography (PET/CT) and multi-parametric magnetic resonance imaging (MRI) in the evaluation of tumor extension of primary prostate cancer. *Transl Androl Urol.* 2020;9:382–390.
36. Grubmüller B, Baltzer P, Hartenbach S, et al. PSMA ligand PET/MRI for primary prostate cancer: staging performance and clinical impact. *Clin Cancer Res.* 2018; 24:6300–6307.
37. Muehlematter UJ, Burger IA, Becker AS, et al. Diagnostic accuracy of multiparametric MRI versus ^{68}Ga-PSMA-11 PET/MRI for extracapsular extension and seminal vesicle invasion in patients with prostate cancer. *Radiology.* 2019; 293:350–358.
38. Thalgott M, Düwel C, Rauscher I, et al. One-stop-shop whole-body ^{68}Ga-PSMA-11 PET/MRI compared with clinical nomograms for preoperative T and N staging of high-risk prostate cancer. *J Nucl Med.* 2018;59:1850–1856.
39. Priester A, Natarajan S, Khoshnoodi P, et al. Magnetic resonance imaging underestimation of prostate cancer geometry: use of patient specific molds to correlate images with whole mount pathology. *J Urol.* 2017;197: 320–326.
40. Priester A, Wu H, Khoshnoodi P, et al. Registration accuracy of patient-specific, three-dimensional-printed prostate molds for correlating pathology with magnetic resonance imaging. *IEEE Trans Biomed Eng.* 2019;66: 14–22.
41. Wu HH, Priester A, Khoshnoodi P, et al. A system using patient-specific 3D-printed molds to spatially align in vivo MRI with ex vivo MRI and whole-mount histopathology for prostate cancer research. *J Magn Reson Imaging.* 2019;49:270–279.